International Journal of Engineering Research and Development

DOI: 10.29137/ijerad.1608652

Volume:17 Issue:2 Pages:416-431 July/2025

Research Article

Investigation of the Mechanical and Wear Behavior of 1.0411 Steel Subjected to Gas Carburizing and Nitriding Processes

Bünyamin Yamanel[1], **Osman Bican**[1]

[1]Mechanical Engineering, Kırıkkale University, Yahsihan/Kırıkkale, 71450, TÜRKİYE

Received: 27/12/2024 **Accepted**: 09/04/2025 **Published Online:** 01/07/2025
Final Version: 15/07/2025

Abstract

In this study, the microstructure, hardness, and wear behavior of 1.0411 steel were investigated after undergoing gas carburizing and nitriding processes. The gas carburizing process was performed using propane gas, while the nitriding process was carried out using pure NH3 gas at 520 °C. After gas carburizing, the samples were subjected to austenitizing at 850 °C for 25 minutes, followed by quenching in water at 60 °C. The process steps were completed by tempering at 140 °C for 25 minutes. Hardness measurements revealed that the surface hardness reached 841±15 HV0.3 after gas carburizing and 429±28 HV0.3 after nitriding. SEM images of the wear surfaces were taken to determine the wear mechanisms. It was found that the gas carburizing process increased wear resistance by 2 times, while the nitriding process increased it by 2.5 times.

Keywords

Gas carburizing, Nitriding, Wear, SEM

**** Corresponding Author:*** ***bunyaminyamanel@hotmail.com***

1. Introduction

AISI 1.0411 steel is widely used in the main shafts of large-section machine tools, medium-hard and wear-resistant gears, hardened pins, and chains. This type of steel is exposed to significant wear depending on its areas of use. Wear reduces the service life of materials, highlighting the importance of surface hardening processes (Chang et al., 2012). The most important surface hardening processes include carburizing, nitriding, aluminizing, chemical vapor deposition (CVD), physical vapor deposition (PVD), and multi-ion arc coating. Among these processes, carburizing and nitriding, which alter the chemical composition of the surface, are more commonly used. Boriding processes provide the highest hardness (Krukovich et al., 2016; Türkmen et al., 2020; Jurči & Hudáková, 2011), excellent wear resistance (Krukovich et al., 2016; Cárdenas, 2016; Joshi, 2015), and corrosion resistance (Davis, 2002; Kulka & Castro, 2019; Przybyłowicz, 2021).

(Girisken & Çam, 2023) determined that the boride layers obtained through the boriding process exhibited high wear resistance at both room temperature and 500 °C, compared to the untreated sample, due to their high hardness and self-lubricating properties.
(Girisken & Çam, 2022) subjected the cobalt-based Haynes 25 superalloy to the boriding process. As a result of the process, they measured the hardness values of the boride layer to be 1890-2454 HV0.1.

Günen et al. (Günen et al., 2023), determined the hardness value of the boride layer obtained through the boriding process to be 20 GPa.

Bölükbaşı et al. (Bölükbaşı et al., 2023), applied a pack aluminum coating process to Inconel 625 material at 700 °C for 3 hours.

It has been determined that the aluminization process can improve the mechanical properties and enhance oxidation resistance.

Gürol et al. (Gürol et al., 2023) determined that by applying an aluminization process to stainless steel material at 1000 °C, they were able to improve the oxidation resistance from 40% to 70%.

Yamanel et al. (Yamanel et al., 2023) determined the surface hardness value to be 2224 HV0.05 after a 4-hour solid boriding process conducted at a temperature of 950 °C.

Hüsem (Hüsem, 2023), has subjected Ti6Al4V steel to the boriding process. It has been determined that the coating thickness increased with the extended boriding time. As the coating thickness increased, wear depths and wear rates showed better results.

(Bayça & Efe, 2022) subjected the 21NiCrMo2 steel to boronizing for different durations. As a result of the corrosion tests, it was found that the corrosion rate of the untreated samples was 491 mm/year, while the corrosion rate of the boronized samples was 323 mm/year.

Carburizing is a process in which carbon diffuses into the surface of low-carbon steels at specific temperatures (above the austenite phase temperature, typically 850-1000 °C) and durations. The carbon content at the surface varies depending on the process temperature, duration, and the carbon content of the carburizing environment (Davis, 2002). In the machinery and manufacturing industry, it can be applied in different forms: solid, liquid, and gas (Yegen, 2009). A carbon-rich protective environment is created in the process, enabling the diffusion of carbon atoms. Afterward, the part is quenched in water to harden the surface. However, regardless of the type of carbon donor medium, the transport of carbon occurs in the gas phase. The carburizing depth may also vary depending on the carbon donor medium used (Tang et al., 2022).

In gas carburizing, the goal is to transfer carbon atoms to the steel surface in an atmospheric environment, to form chemical reactions on the surface, and consequently, to accumulate carbon atoms on the steel surface. There are three key reactions that determine the rate of carbon transfer to the steel surface during carburizing reactions (Collin et al., 1972):

$$2CO \rightarrow C + CO_2 \tag{1}$$

$$CH_4 \rightarrow C + 2H_2 \tag{2}$$

$$CO + H_2 \rightarrow C + H_2 \tag{3}$$

In the carburizing process, CO gas continues to dissociate rapidly, while the CO_2 gas formed as a result of the reaction causes decarburization. This, in turn, reduces the strength and fatigue resistance of the steel (Collin et al., 1972). The primary goal of the carburizing process is to form a hard layer on the surface. By rapidly cooling the parts, a phase known as martensite is formed on the surface, thereby increasing wear and fatigue resistance (Krauss, 1991). Another factor affecting surface hardness is the process duration. As the duration increases, more austenite remains in the martensitic structure, which reduces surface hardness (Ihom, 2013; Schneider & Chatterjee, 2013; Yegen, 2009).

A disadvantage of the carburizing process is the non-homogeneous formation of the carbide layer on the surface and its oxidation (Ryzhov et al., 2010). To remove the oxidation that occurs on the surface as a result of gas carburizing, grinding is performed. However, this creates additional stresses and cost issues on the steel material. A new technology is emerging that allows precise control over the morphology, size, and surface layer depth of the carbide structure. Fatigue analysis of helical gears has been applied to various steels (Gawroński et al., 2010; Wang et al., 2019). This process is carried out in vacuum furnaces under low pressure and at high temperatures. Gases such as C_2H_2, C_3H_8, and C_2H_4 are used in this application. The reactions that occur in this process are provided below (Davis, 2002; Karagöz, 2007).

$$C_2H_2 \rightarrow 2C + H_2 \tag{4}$$

$$C_3H_8 \rightarrow CH_4 + C_2H_4 \tag{5}$$

$$C_2H_4 \rightarrow C + CH_4 \tag{6}$$

The nitriding process is a thermo-chemical treatment based on the diffusion of nitrogen atoms into the material surface, leading to the formation of nitride phases (Arif et al., 2010). It can be applied in different forms, including gas, plasma, and salt bath methods. The process duration may vary depending on the material thickness and the desired nitriding depth (Lampman, 1995).

Among these methods, gas nitriding involves the controlled introduction of nitrogen into the furnace at an appropriate temperature, where nitrogen diffuses into the material. Ammonia (NH_3) is typically used as the gas in this process. The process temperature ranges from 490 to 580 °C. Gas nitriding is considered the best method for the homogeneous nitriding of complex-shaped parts (Hernandez et al., 2008; O'Brien, 1995). Compared to alternative surface hardening techniques such as carburizing and carbonitriding, nitriding is applied at lower temperatures. A white layer forms on the surface.

During the nitriding process, no cooling is required, which minimizes distortions (Rodrigo et al., 2010; Karcan, 2005). Using NH_3, nitrogen atoms are separated and react with iron and alloying elements to form fine-grained nitrides (the white layer) (Güven et al., 2014).

$$2NH_3 \rightarrow N_2 + 3H_2 \tag{7}$$

The white layer contributes to the improvement of corrosion properties, while the diffusion layer enhances the tribological properties and fatigue resistance of steels (Birol &Yuksel, 2012).

In the nitrogen diffusion zone, nitrogen exists as an interstitial atom in a cubic iron structure or as finely dispersed alloy nitrides. The hardness value decreases as the nitrogen content in the inner parts of the steel decreases (Baranowska, 2010). The nitriding process is widely used to improve the tribological properties of surfaces (Da Silva et al., 2007).

In the nitriding process, a nitride layer is formed, creating a hard surface layer (Özcan, 2012).

Pekgöz et al. (Pekgöz et al., 2013), applied liquid carburizing to AISI 8620, AISI 4140, and AISI 1040 steels. After carburizing, surface hardness measurements and microstructure examinations were performed. The 1040 steel was carburized for 2 hours at 845 °C, the 4140 steel for 4 hours at the same temperature, and the 8620 carburizing steel for 4 hours at 900 °C in a liquid medium. The samples were quenched and then subjected to tempering at 250 °C for 2 hours.

In their study, Erkan et al. (Erkan et al., 2020), applied gas carburizing to AISI 8620 steel. The carburizing processes were performed at 920 and 980 °C. It was found that the carburizing depth increased with higher temperatures.

In this study, 1.0411 steel, which is commonly used in the machinery manufacturing industry, was subjected to gas carburizing and nitriding processes. 1.0411 steel is a low-carbon, non-alloyed steel. Gas carburizing is generally applied to carburizing steels, while nitriding is used for alloy steels. A review of the literature shows that there is limited research on the carburizing and nitriding of this type of steel. Given that 1.0411 steel is exposed to significant wear depending on its applications, this study aimed to contribute to the literature by examining the microstructure, hardness, and wear properties of 1.0411 steel subjected to gas carburizing and nitriding processes.

Symbols and Abbreviations

k	Wear coefficient
W	Volume loss(mm^3)
F	Applied force(N)
s	Sliding distance(m)
NH_3	Ammonia
Al_2O_3	Aluminum oxide
SEM	Scanning electron microscope
AISI	American iron and steel institute
CO	Carbon monoxide
CO_2	Carbon dioxide
CH_4	Methane
C_2H_4	Ethylene
C_3H_8	Propane
N_2	Nitrogen
H_2	Hydrogen

2. Materials and Methods

For the gas carburizing and nitriding processes, cylindrical 1.0411 steel was obtained from the market. The samples were prepared by machining to a diameter of 12 mm and a length of 18 mm.

2.1 Chemical Composition and Microstructural Analysis

Chemical analysis of the experimental samples was performed using the optical emission argon spectrometry method. Prior to the gas carburizing process, the samples were preheated at 600 °C for 1 hour and 20 minutes. Gas carburizing was then performed at 910 °C for 5 hours using propane gas. After gas carburizing, the samples were austenitized at 850 °C for 25 minutes, followed by quenching in oil at 60 °C. The process was completed by tempering at 140 °C for 25 minutes. A schematic overview of the gas carburizing process steps is shown in Figure 1.

Table 1. Gas carburizing and nitriding process parameters

Process temperature(°C)	Process duration(h)	Thermochemical process
910	5	Gaz carburizing
520	5	Nitriding

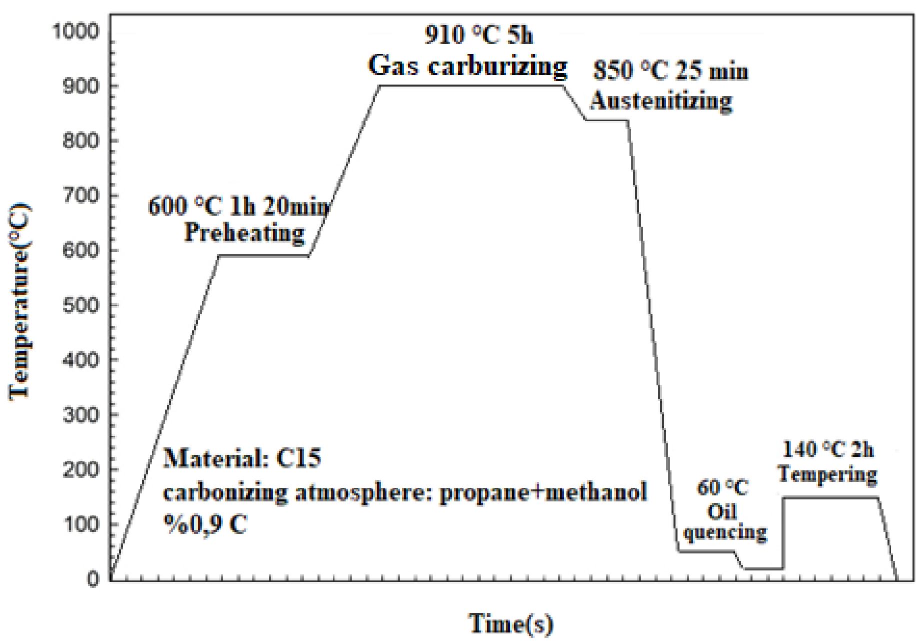

Figure 1. Steps of the gas carburizing process

The samples to be nitrided were preheated at 350 °C. Nitriding was then applied using pure NH_3 gas at 520 °C for 5 hours. After nitriding, the samples were tempered at 400 °C for 2 hours. A schematic representation of the nitriding process is shown in Figure 2. The samples, which were cooled in still air, were cut using a precision saw and mounted in bakelite. The mounted samples were then subjected to polishing with alumina abrasives of 200, 400, 600, 800, and 1000 grit. Subsequently, the sample surfaces were polished using polishing solutions of 9, 6, 3, and 1 µm. The sample surfaces were etched with a 2% nital solution, and SEM and optical images of the microstructure were obtained.

The XRD analysis was performed at a scanning speed of 2 degrees, in 2theta/theta mode, continuous scanning mode, and with a sampling width of 0.200 degrees.

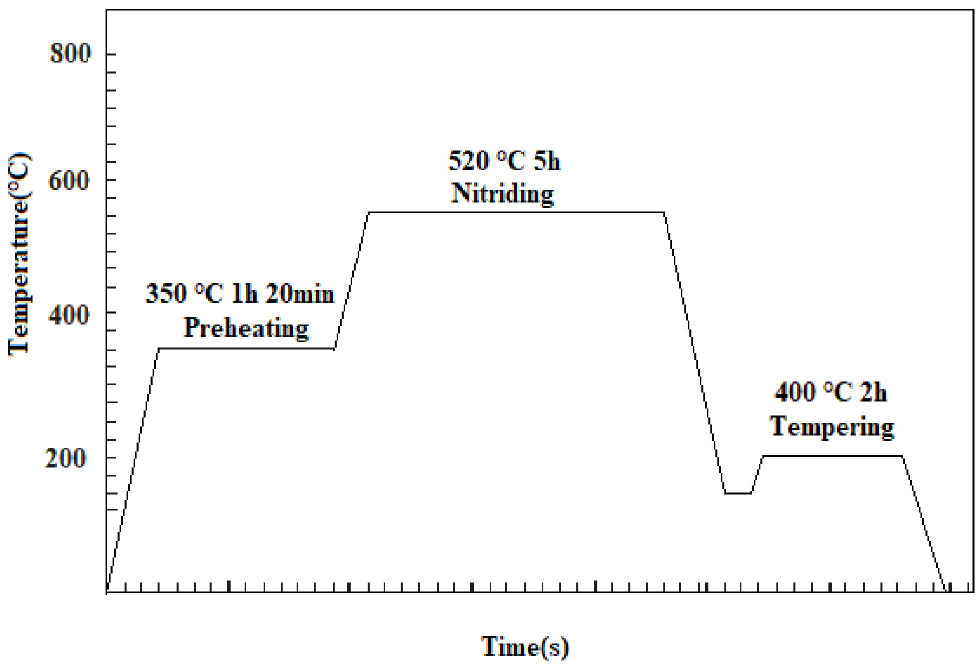

Figure 2. Steps of the nitriding process

A schematic representation of the diffusion is shown in Figure 3.

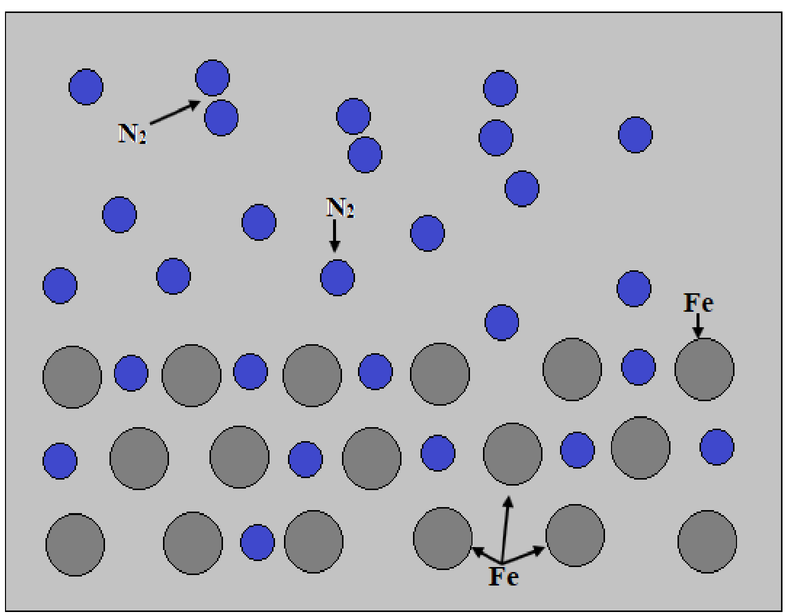

Figure 3. Schematic view of nitriding diffusion(Yang, 2012)

2.2 Hardness Measurements

Hardness measurements of the samples were performed using the Vickers hardness test method, with a 300 g load, at intervals of 50 µm from the surface to the inner part of the sample.

2.3 Wear Tests

The samples were subjected to abrasive wear testing. A schematic of the testing device used for the wear tests is shown in Figure 4. The wear tests were conducted at a sliding speed of 0.5 m/s and a sliding distance of 40 m. Alumina (Al_2O_3) abrasive papers with a diameter of 200 mm and a grit size of 66 µm were used as the abrasive. The wear tests were performed with three different loads: 10 N, 30 N, and 50 N.

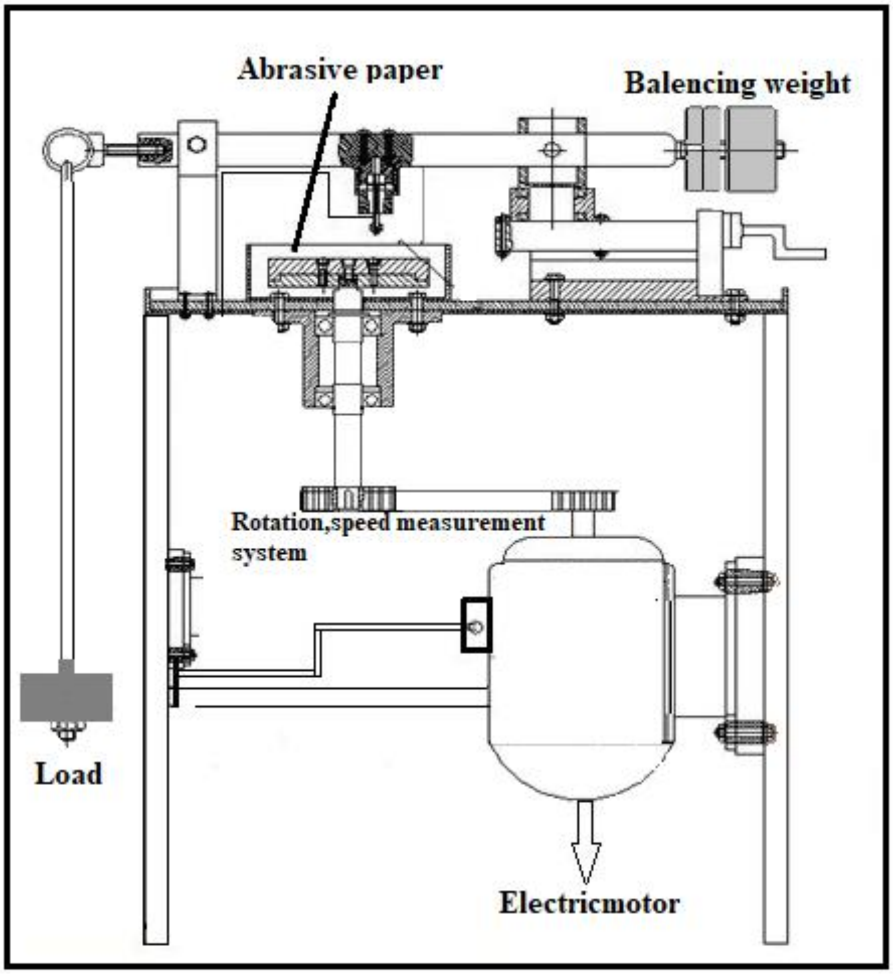

Figure 4. Schematic view of the wear testing apparatus

Table 2. Wear Test Parameters

Sliding velocity (m/s)	Load (N)	Type of abrasive	Abrasive size (µm)
0.5	10, 30 ve 50	Al_2O_3	66

The samples subjected to wear tests were cleaned before and after the tests using a special cleaning agent. The weight losses of the cleaned samples were determined using a precision balance with an accuracy of 0.0001. The calculated weight losses were divided by the sample density to determine the volume losses.

2.4 Wear Coefficient Calculation

The wear coefficients were determined using the equation provided in Equation 7.

$$k = \frac{W}{Fn.s} \tag{8}$$

Here, W is the volume loss (mm³) resulting from wear, Fn is the applied force (N), and s (m) is the sliding distance.

3. Results and Discussion

3.1 Chemical Composition and Microstructural Analysis

Table 3. Chemical composition of 1.0411 steel

Element	C	Mn	P	S	Si	Cr	Fe
% Composition	0.213	0.44	0.04	0.045	0.4	-	Denge

In the optical image of the microstructure of 1.0411 steel shown in Figure 5, it has been observed that the microstructure consists of ferrite and pearlite phases. Figure 6 shows the SEM images of 1.0411 steel subjected to gas carburizing and nitriding. Upon examining Figure 6, it has been determined that a carbide layer is formed on the sample subjected to gas carburizing, while a nitride layer forms on the sample subjected to nitriding.

In the study by Pekgöz et al. (Pekgöz et al., 2013), after liquid carburizing, the microstructure of AISI 1040 steel showed pearlite and cementite, while carbide components, bainite, and martensite were observed in the microstructure of a low-alloy steel.

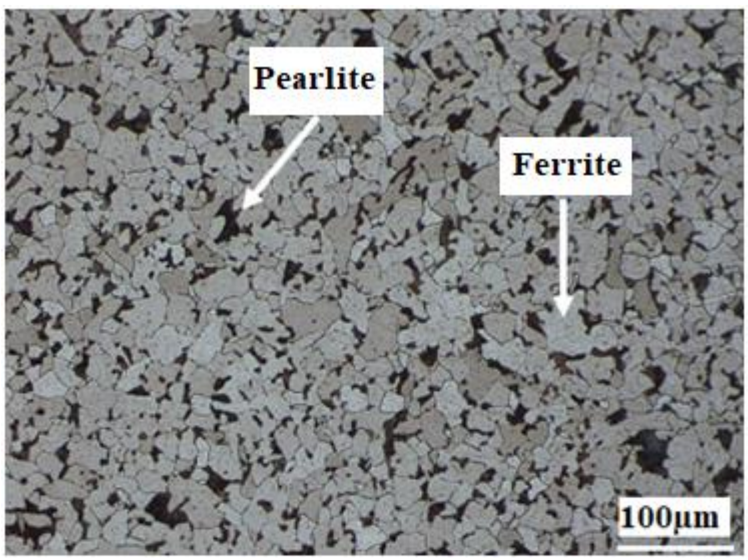

Figure 5. Optical image of the microstructure of 1.0411 steel

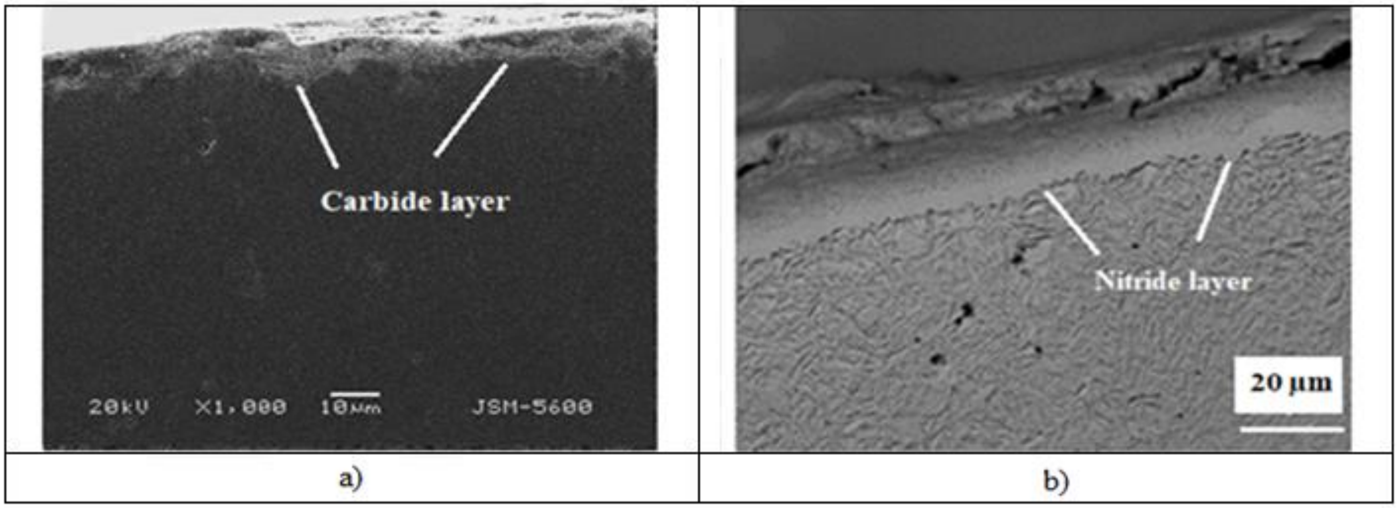

Figure 6. (a) SEM image of gas carburizing 1.0411 steel; **(b)** SEM image of nitriding 1.0411 steel

The XRD analysis results of nitriding 1.0411 steel are shown in Figure 7. Upon examining the graph, it was determined that α-Fe and $Fe_3N_{1.3}$ phases have formed in the structure.

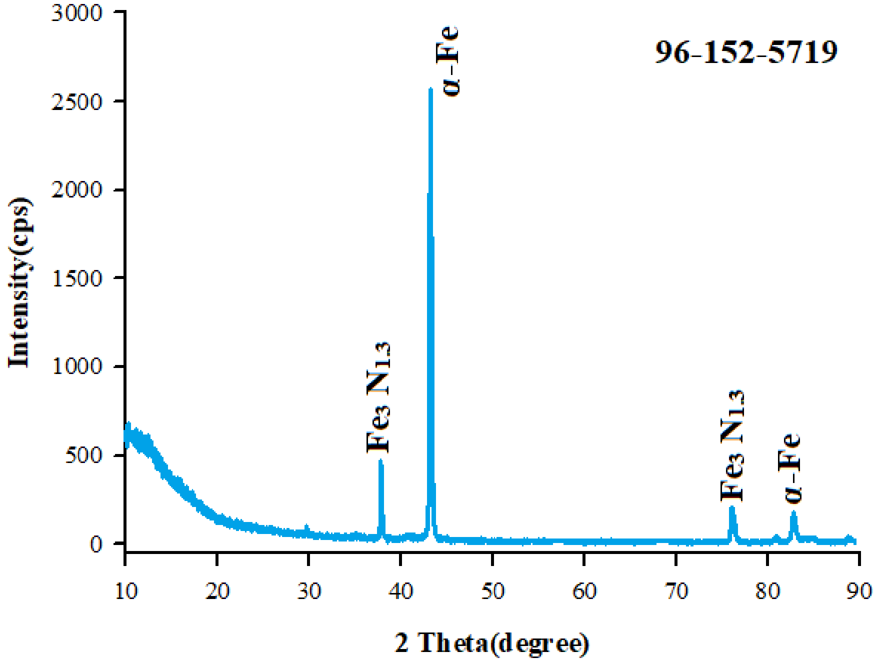

Figure 7. XRD analysis of nitrided 1.0411 steel

3.2 Hardness Measurements

The core hardness of 1.0411 steel was determined to be 250-270±10 HV0.3 based on the measurements. Upon examining the hardness graph shown in Figure 8, it was found that the highest hardness values were observed in the samples subjected to gas carburizing. This can be explained by the accumulation of carbon atoms on the surface during the gas carburizing process. The accumulation of carbon atoms on the surface, influenced by temperature and time, increased the hardness values. As the measurement progressed from the surface towards the core, a decrease in hardness values was observed. This can be explained by the reduction in the diffusion of carbon atoms towards the inner region. After gas carburizing, the hardness values in the carbide region on the surface were found to range between 734-841±15 HV0.3. It was determined that the gas carburizing process increased the hardness values by 3 times.

When examining the hardness values of the nitrided steel, it was found that the hardness values in the nitride layer ranged from 407-429±28 HV0.3. The nitriding process increased the core hardness by approximately 2 times.

Hardness values decreased towards the inner part of the sample. This can be explained by the formation of hard phases on the surface as a result of the nitriding process. The reduction in the diffusion of nitrogen towards the inner region causes a decrease in the hardness values.

Güven et al. (Güven et al., 2014), applied nitriding to AISI 4140 steel for two different durations, 18 and 19.5 hours. The core hardness of the steel was 221 HV, while after nitriding, the hardness was measured as 522 HV and 557 HV, respectively.

Pekgöz et al. (Pekgöz et al., 2013) determined that the surface hardness values increased by 2 times as a result of the liquid carburizing process. It was found that the microstructure obtained after carburizing had an effect on the hardness.

Erkan et al. (Erkan et al., 2020) in their study found that the surface hardness values of steel increased as a result of the gas carburizing process. Additionally, it was observed that with increasing temperature, the amount of carbon atoms diffusing to the surface also increased, leading to a further increase in hardness values.

Çoşar (Çoşar, 2014), in his study, subjected 20MnCr5 and 8622RH steels to gas carburizing. The hardness values of the materials before the process were 19-20 HRC, and after the process, the hardness values increased to 57.3 HRC for 20MnCr5 steel and 60.5 HRC for 8622RH steel, respectively.

When examining similar studies in the literature (Nitriding, liquid carburizing, and gas carburizing), it has been determined that the surface hardness values significantly increase as a result of these processes. This is believed to be related to the carbon and nitrogen atoms that diffuse into the surface through nitriding and carburizing processes. It is thought that factors such as processing time, material type, and temperature play a significant role in the hardness values. Güven et al. (Güven et al., 2014) found that the surface hardness obtained through nitriding of the 1.0411 steel was higher than the hardness value obtained from nitriding of another steel type. This difference is thought to be due to the varying types of steel and processing times. Pekgöz et al. (Pekgöz et al., 2013) reported that the hardness increase obtained through liquid carburizing was limited compared to the hardness increase observed in the present study.

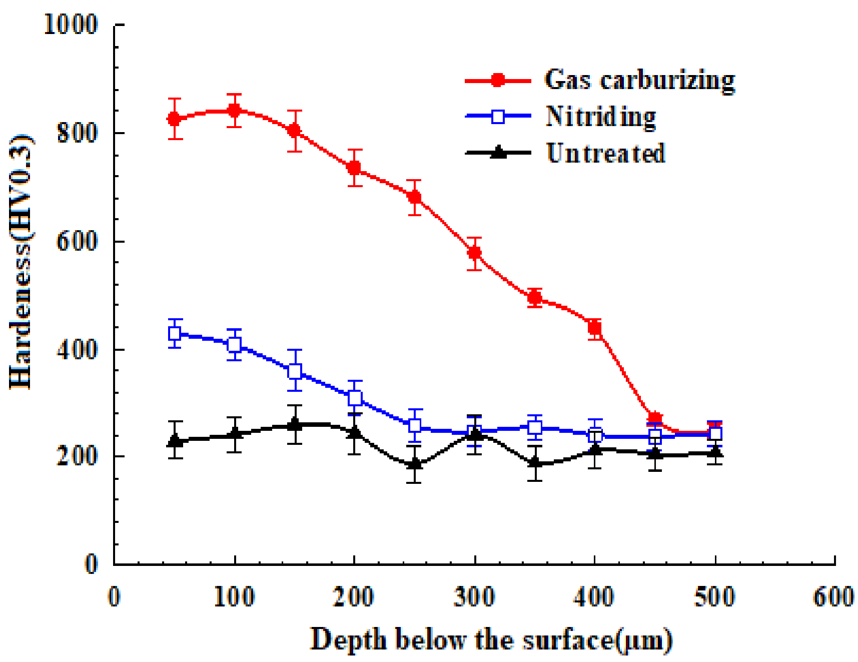

Figure 8. Variation of hardness values of gas carburizing and nitriding 1.0411 steel with respect to sub-surface distance

3.3 Wear Tests

The wear surfaces of the untreated, gas carburizing, and nitriding samples were examined using SEM analysis. The SEM images of the wear surfaces are provided in Figures 9-11.

When examining the wear surfaces of the untreated samples (Figure 9), it was found that there were particles detached from the surface, pits, and areas subjected to plastic deformation. This can be explained by the low hardness values of the material. The effect of the Al_2O_3 abrasive, which has high hardness, under a specific sliding speed and load, causes relative motion that leads to the detachment of particles from the surface.

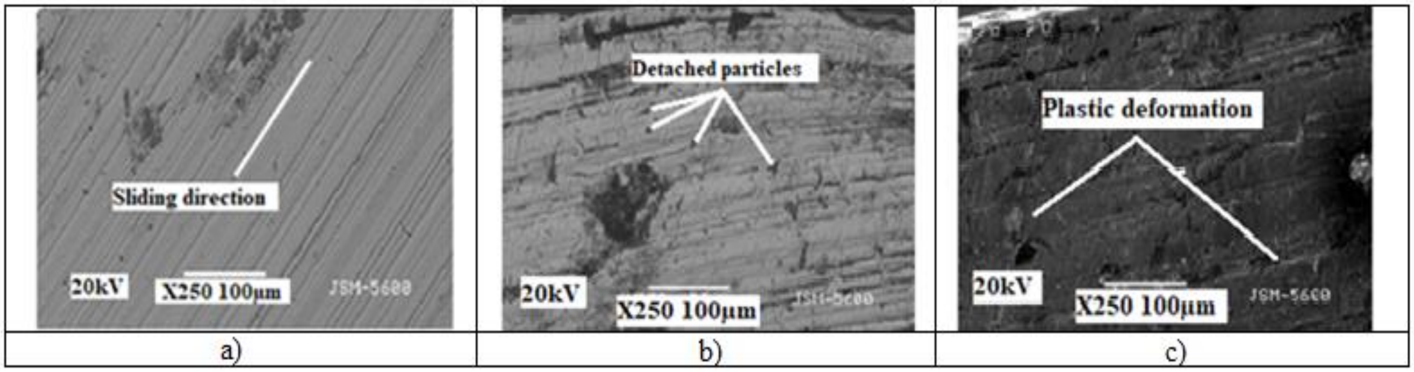

Figure 9. SEM images of the worn surface of untreated steel after wear tests using a 66 µm abrasive under **(a)** 10N; **(b)** 30N; **(c)** 50N loads

When examining the wear surfaces of the gas carburizing and nitriding samples, it was observed that the number of pits on the surface had decreased. This is due to the increase in surface hardness resulting from the thermochemical treatments. The carbon atoms accumulated on the surface as a result of gas carburizing and the hard layer formed on the surface due to nitriding directly affect the hardness. The increased surface hardness makes the samples more resistant to abrasive wear. SEM images of the wear surfaces of the gas carburizing and nitriding samples are shown in Figures 10-11.

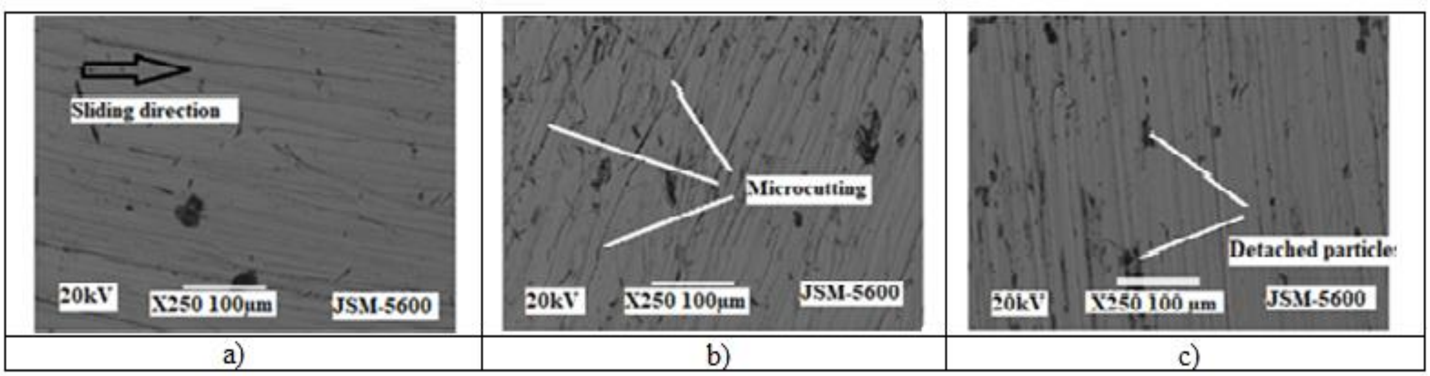

Figure 10. SEM images of the worn surface of the gas carburizing steel after wear tests using a 66 µm abrasive under **(a)** 10N; **(b)** 30N; **(c)** 50N loads

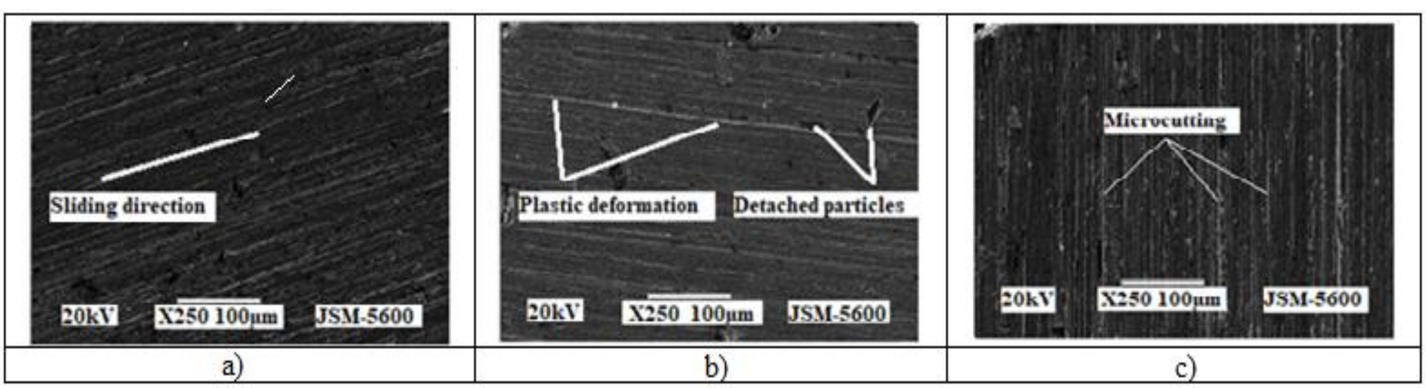

Figure 11. SEM images of the worn surface of nitriding 1.0411 steel after wear tests using a 66 µm abrasive under **(a)** 10N; **(b)** 30N; **(c)** 50N loads

The volume loss graph of the untreated, gas carburizing, and nitriding 1.0411 steel under load is shown in Figure 12. The wear type that occurs is abrasive wear. During the wear process, the samples come into contact with abrasive particles (Al_2O_3), which causes friction. This friction generates heat, which can accelerate the wear process. The high hardness of the abrasive material causes particles to detach from the sample surface, leading to wear. This effect varies depending on the applied force, speed, and the type of material during the wear test. Upon examining Figure 12, it was found that the untreated samples exhibited the highest wear resistance. As the load increased from 10-30 N, the wear also increased. However, in the 30-50 N range, a decrease in wear was observed.

This can be explained as follows: the change in the wear mechanism between 30-50 N is thought to be the cause. The adhesion or embedding of high hardness Al_2O_3 particles into the steel surface can increase wear resistance.

It has been determined that the gas carburizing and nitriding processes improve wear behavior. The increase in hardness values due to the thermal treatments has enhanced the wear resistance. It was observed that wear resistance decreased with increasing force. The best wear resistance was achieved as a result of the nitriding process, where wear resistance increased by 2.5 times.

Gerasimov et al. (Gerasimov et al., 2014) Gerasimov et al. (2014) in their study found that the wear resistance increased with the carburizing process performed at a temperature of 930°C. They emphasized that the activation of the carburizing process led to an improvement in wear resistance. In this study, the increase in wear resistance due to the carburizing process is also observed in Figure 12. This can be explained by the accumulation of carbon atoms on the surface, which is supported by both the literature and the findings of this study. The increase in carbon atoms on the surface enhances the hardness values, which in turn has a positive effect on improving the wear behavior.

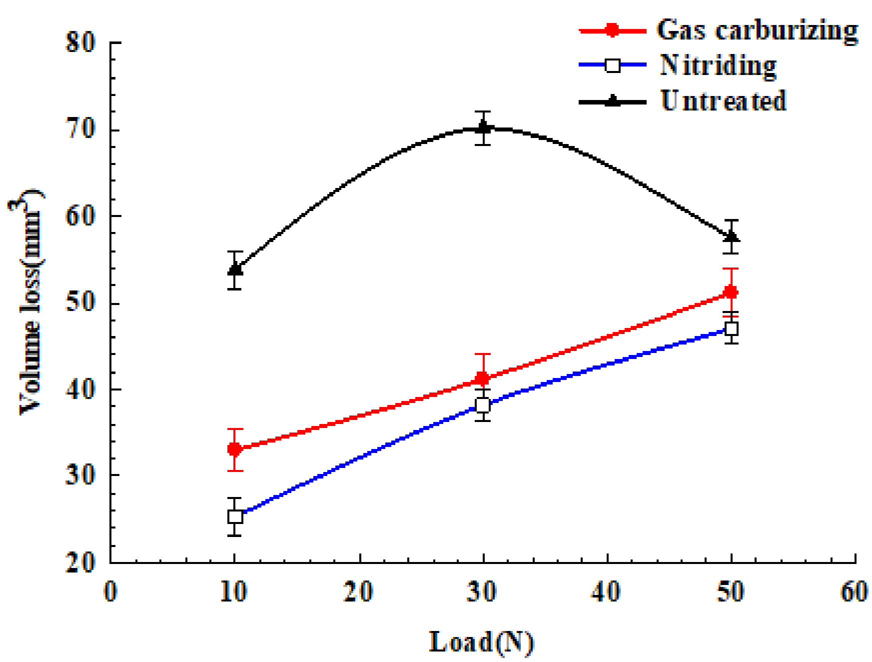

Figure 12. Volume loss vs. load graph after wear

3.4. Wear Coefficient

In Figure 13, the wear coefficient graph with respect to the applied load is presented. It was determined that the untreated samples had the highest wear coefficient. The gas carburizing and nitriding processes applied to the samples were found to reduce the wear coefficient values. The lowest wear coefficient was observed in the nitriding samples. As the load increased, the wear coefficients of all samples became closer to each other. This can be explained as follows: After the gas carburizing and nitriding processes, carbide and nitride layers were formed on the surface (Figure 6). During wear, these layers start to detach under the applied force. In the wear test performed at a 50N load, the detachment of these layers reduced the wear resistance, bringing the wear coefficient values of the treated samples to the same level as those of the untreated samples. It was also observed that the wear coefficient decreased with increasing applied force.

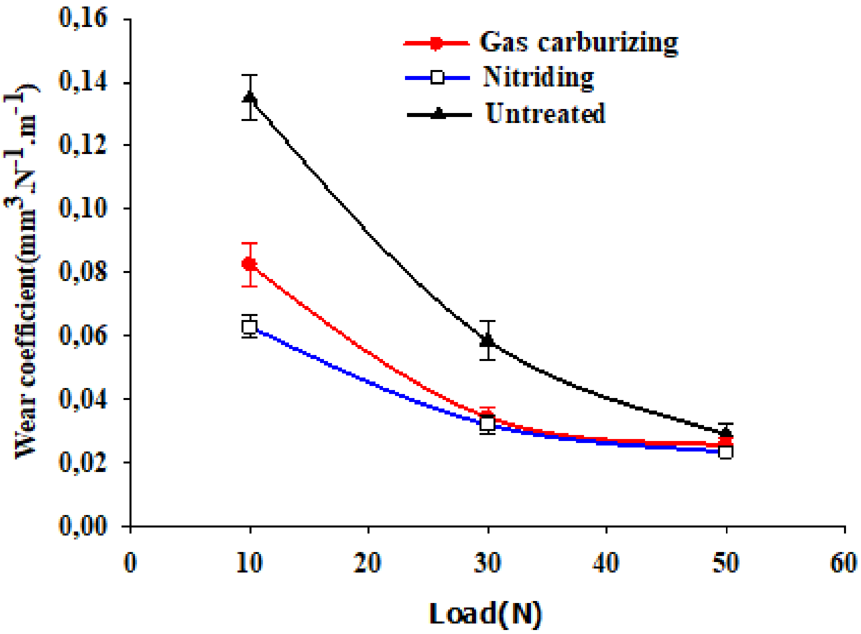

Figure 13. Wear coefficient vs. load graph

4. Conclusion

In this study, gas carburizing and nitriding processes were applied to 1.0411 steel, which is frequently preferred in the machinery and manufacturing industries. The internal structure, hardness, and wear behavior of the steel were experimentally investigated after the processes.

- The internal structure was examined using SEM analysis after gas carburizing and nitriding, and it was found that a carbide layer and a nitride layer were formed on the surface due to carbon diffusion.
- As a result of the hardness measurements, the core hardness of the steel was determined to be 250-270±10 HV0.3, while the hardness of the carbide layer was found to be 734-841±15 HV0.3, and the hardness after nitriding was 429±28 HV0.3. It was determined that the core hardness increased 3 times after gas carburizing and 2 times after nitriding.
- In the wear surfaces of untreated samples, a large number of scratches, pits, and detached particles were observed. When examining the wear surfaces of gas carburizing samples, it was found that the number of scratches had decreased. After nitriding, fine scratches were observed on the wear surfaces.
- When examining the volume loss vs. load graphs after wear, it was found that the highest wear occurred in the untreated sample. It was determined that gas carburizing improved wear behavior by approximately 2 times, while nitriding improved wear behavior by 2.5 times. Wear coefficients were calculated, and the lowest wear coefficients were found in the nitriding samples.

5. References

Arif, A. F. M., Akhtar, S. S., & Yilbas, B. S. (2010). Effect of process variables on gas nitriding of H13 tool steel with controlled nitriding potential. International Journal of Surface Science and Engineering, 4(4), 396–415. https://doi.org/10.1504/IJSSCE.2010.037111.

Baranowska, J. (2010). Importance of surface activation for nitrided layer formation on austenitic stainless steel. Surface Engineering, 26(4), 293–298. https://doi.org/10.1179/174329409X12593687690710.

Bayça, S. U., & Efe, H. (2022). Effects of boriding process on corrosion rate of 21NiCrMo2 steel. International Journal of Engineering Research and Develeopment, 14(1), 1-9. https:// doi.org/10.29137/umagd.1036043.

Birol, Y., & Yuksel, B. (2012). Performance of gas nitrided and AlTiN coated AISI H13 hot work tool steel in aluminium extrusion. Surface and Coatings Technology, 207(1), 461–466. https://doi.org/10.1016/j.surfcoat.2012.06.016.

Bölükbaşı, Ö. S., Serindağ, T., Gürol, U., Günen, A., & Çam, G. (2023). Improving oxidation resistance of wire arc additive manufactured Inconel 625 Ni-based superalloy by pack aluminizing. CIRP Journal of Manufacturing Science and Technology, 46, 89-97. https://doi.org/10.1016/j.cirpj.2023.07.011.

Cárdenas, E. E. V., Lewis, R., Pérez, A. I. M., Ponce, J. L. B., Pinal, F. J. P., Domínguez, M. O., & Arreola, E. D. R. (2016). Characterization and wear performance of boride phases over tool steel substrates. Advances in Mechanical Engineering, 8, 1–10.

Chang, S.-H., Huang, K.-T., & Wang, Y.-H. (2012). Effects of thermal erosion and wear resistance on AISI H13 tool steel by various surface treatments. Materials Transactions, 53(4), 745–751.

Collin, R., Gunnarson, S., & Thulin, D. (1972). Mathematical model for predicting carbon concentration profiles of gas-carburized steel. Journal of the Iron and Steel Institute, 210(10), 785–789.

Coşar, D. (2014). Investigation of the effect of gas carburizing process on wear and mechanical properties of 8622RH and 20MnCr5 steels. (Master's thesis). Eskisehir Osmangazi University, Eskişehir, Turkey.

Da Silva, L. L. G., Ueda, M., & Nakazato, R. Z. (2007). Enhanced corrosion resistance of AISI H13 steel treated by nitrogen plasma immersion ion implantation. Surface and Coatings Technology, 201, 8291–8294. https://doi.org/10.1016/j.surfcoat.2006.11.020.

Davis, J. R. (2002). Boriding. In Surface hardening of steels (pp. 213–226). ASM International.

Davis, J. R. (2002). Surface hardening of steels: Understanding the basics. ASM International, Materials, 91.

Erkan, A., Yılmaz, Ü., Helvacıoğlu, Ş., Günay, H., Aydoğan, R., & Ersoy, Ç. (2020). Improvement of mechanical and metallographic properties of materials by low pressure cementation method. Mühendis ve Makine.

Gawroński, Z., Malasiński, A., & Sawicki, J. (2010). Elimination of galvanic copper plating process used in hardening of conventionally carburized gear wheels. International Journal of Automotive Technology, 11, 127–131.

Gerasimov, S. A., et al. (2014). Mechanical properties of hot-working steels after activization of cementation process. Journal of Mechanical Engineering and Manufacturing Reliability, 43(4), 322–326.

Girisken, I., & Çam, G. (2023). Characterization of microstructure and high-temperature wear behavior of pack-borided Co-based Haynes 25 superalloy. CIRP Journal of Manufacturing Science and Technology, 45, 82-98. https://doi.org/10.1016/j.cirpj.2023.06.012.

Girişken, İ., & Çam, G. (2022). Boriding of cobalt-based Haynes 25/L-605 superalloy. Journal of Characterization. https://doi.org/10.29228/JCHAR.66388.

Günen, A., Gürol, U., Koçak, M., & Çam, G. (2023). Investigation into the influence of boronizing on the wear behavior of additively manufactured Inconel 625 alloy at elevated temperature. Progress in Additive Manufacturing, 8, 1281-1301. https://doi.org/10.1007/s40964-023-00398-8.

Gürol, U., Altınay, Y., Günen, A., Bölükbaşı, Ö. S., Koçak, M., & Çam, G. (2023). Effect of powder-pack aluminizing on microstructure and oxidation resistance of wire arc additively manufactured stainless steels. Surface & Coating Technology, 468, 129742. https://doi.org/10.1016/j.surfcoat.2023.129742.

Güven, Ş. Y., Delikanlı, K., & Öncel, E. (2014). Effect of ion nitriding surface hardening treatment applied to AISI 4140 steel on fatigue strength. SDU Technical Sciences Journal, 4, 29-39.

Hernandez, M. H. S. M., Staia, M. H., & Puchi-Cabrera, E. S. (2008). Evaluation of microstructure and mechanical properties of nitrided steels. Surface and Coatings Technology, 202, 1935-1943.

Hüsem, F. (2023). The effects of boriding at 800°C at different times on Ti6Al4V. International Journal of Engineering Research and Development, 15(2), 881-890. https://doi.org/10.29137/umagd.1306808.

Ihom, P. A. (2013). Case hardening of mild steel using cowbone as energiser. African Journal of Engineering Research, 1(4), 97-101.pp. 97-10.

Joshi, A. A., Hosmani, S. S., & Dumbre, J. (2015). Tribological performance of boronized, nitrided, and normalized AISI 4140 steel against hydrogenated diamond-like carbon-coated AISI D2 steel. Tribology Transactions, 58(3), 500–510.

Jurči, P., & Hudáková, M. (2011). Diffusion boronizing of H11 hot work tool steel. Journal of Materials Engineering and Performance, 20(7), 1180–1187.

Karagöz, İ. (2007). Investigation of heat treatment conditions that will increase diffusion and hardness depth in case hardening steels. (Master's thesis). Marmara University, İstanbul, Turkey.

Karcan, F. (2005). Study of the life of hot work valve molds (Master's thesis). İstanbul Technical University, İstanbul, Turkey.
Krauss, G. (1991). Metals handbook (pp. 363-375). ASM International.

Krukovich, M. G., Prusakov, B. A., & Sizov, I. G. (2016). Plasticity of boronized layers. Springer International Publishing.

Kulka, M., & Castro, M. (2019). Current trends in boriding. Springer International Publishing. https://doi.org/10.1007/978-3-030-06782-3.

Lampman, S. (1995). Introduction to surface hardening of steels. ASM Handbook, Heat Treating, 4, 607-619.

O'Brien, J. M. (1995). Plasma (ion) nitriding of steels. ASM Handbook, Heat Treating, 4, 944-954.

Özcan, H. (2012). Development of a new heat treatment method to increase the wear resistance of 32CrMoV Steel (Master's thesis, Hacettepe University). Hacettepe University Institute of Science and Technology, Ankara, Turkey.

Pekgöz, B., Sarıdemir, S., Uygur, İ., & Aslan, Y. (2013). Effects of cementation process on microstructure and hardness values of different steels. Machine Technologies Electronics Magazine, 10(1), 19-24.

Przybyłowicz, K. (2021). Teoria i praktyka borowania stali. Wydawnictwo Politechniki Śląskiej.

Rodrigo, L. O. B., Heloise, O. P., Vanessa, S., Israel, J. R. B., Silvia, A. C. A., Fernando, S. de S., Almir, S., Carlos, A. F., & Cristiano, G. (2010). Microstructure and corrosion behaviour of pulsed plasma-nitrided AISI H13 tool steel. Corrosion Science, 52, 3133–3139.

Ryzhov, N. M., Fakhurtdinov, R. S., & Smirnov, A. E. (2010). Cyclic strength of steel 16Kh3NVFBM-Sh (VKS-5) after vacuum carburizing. Metal Science and Heat Treatment, 52, 61–66.

Schneider, M. J., & Chatterjee, M. S. (2013). Introduction to surface hardening of steels. ASM Handbook, Volume 4A, 259–267. ASM International.

Tang, Y., Zhang, G., Mao, H., Ren, J., Huang, Z., Li, X., & Li, Q. (2022). Research on the sensor for detection of carburized case depth based on nonlinear ultrasound. Results in Physics, 42, 105984.

Türkmen, İ., Yalamaç, E., & Keddam, M. (2020). Investigation of tribological behaviour and diffusion model of Fe_2B layer formed by pack-boriding on SAE 1020 steel. Surface & Coatings Technology, 380, 125154. https://doi.org/10.1016/j.surfcoat.2019.08.017.

Wang, H., Wang, B., Wang, Z., Tian, Y., & Misra, R. D. K. (2019). Optimizing the low-pressure carburizing process of 16Cr3NiWMoVNbE gear steel. Journal of Materials Science and Technology, 35(7), 1218–1227.

Yang, M. (2012). Nitriding—Fundamentals, modeling, and process optimization (Doctoral dissertation, Worcester Polytechnic University). Worcester Polytechnic University, USA.

Yamanel, B., Bican, O., & Bayça, S. U. (2023). Investigation of internal structure and hardness behavior of AISI 1020 steel subjected to surface hardening process using Baybora-2 boriding powder. International Journal of Engineering Research and Development, 15(1), 164-171. https://doi.org/10.29137/umagd.1174515.

Yegen, İ. (2009). Effect of salt bath cementation process on wear resistance of hot rolled and cold drawn SAE 8620 and 16MnCr5 steels (Master's thesis). Gebze Institute of Technology, Gebze, Kocaeli.